



Cite this: DOI: 10.1039/c7gc02991h

Received 3rd October 2017,
Accepted 27th November 2017

DOI: 10.1039/c7gc02991h

rsc.li/greenchem

Synergistic effects in Fe nanoparticles doped with ppm levels of (Pd + Ni). A new catalyst for sustainable nitro group reductions†

Haobo Pang,^a Fabrice Gallou,^b Hyuntae Sohn,^c Jeffrey Camacho-Bunquin,^c Massimiliano Delferro^c and Bruce H. Lipshutz^{c,*a}

A remarkable synergistic effect has been uncovered between ppm levels of Pd and Ni embedded within iron nanoparticles that leads to mild and selective catalytic reductions of nitro-containing aromatics and heteroaromatics in water at room temperature. NaBH₄ serves as the source of inexpensive hydride. Broad substrate scope is documented, along with several other features including: low catalyst loading, low residual metal in the products, and recycling of the catalyst and reaction medium, highlight the green nature of this new technology.

Introduction

Bimetallic catalysis is a blossoming area of synthetic organic chemistry, potentially offering tremendous opportunities that augment traditional metal-catalyzed processes.¹ As recently reviewed by Pye and Mankad,² both mixed metal and multi-valent, single metal catalysts have led to exciting C–C and C–X couplings, while selected oxidations using related species have also been highlighted this year as well by Parmeggiani, Matassini, and Cardona.³ Missing from these discussions are applications of synergistic effects to multiple metal-catalyzed processes in general, and to nitro group reductions, in particular. Development of a highly efficient new technology that not only takes advantage of two transition metals working in harmony towards a common synthetic goal, but also adheres to many of the 12 Principles of Green Chemistry⁴ would be of special merit. In this report we describe a newly discovered synergistic relationship between two group 10 metals. That is, very clean reduction of aromatic and heteroaromatic nitro groups to the corresponding primary amines takes place in

water at room temperature when *ppm levels of both* Pd and Ni are embedded within iron nanoparticles.

Selective reduction of nitro groups represents an essential methodology, given the importance of this functional group within intermediates for fine chemicals, agrochemicals, pharmaceuticals, dyes, and polymers.⁵ In general, reductions of nitroarenes tend to be either metal-free or metal-based.⁶ The latter category tends to rely on precious metals such as Pd,⁷ Au,⁸ Ru,⁹ Pt¹⁰ and In,¹¹ or non-noble metals such as Co,¹² Ni,¹³ Mo,¹⁴ Zn,¹⁵ Ti¹⁶ and Fe.¹⁷ Although hydrogenation has been the most widely used approach, issues such as the need for high pressure equipment, flammable hydrogen gas, and relatively high loadings of expensive metals that oftentimes can localize as residual metal in the product remain. Environmental concerns stemming in large measure from organic waste that is mainly attributed to organic solvents¹⁸ can add to the unattractiveness of such traditional approaches.

In previous work from our group,¹⁹ it was found that commercial sources of FeCl₃ augmented with only 80 parts per million (ppm) Pd, upon processing into nanoparticles (NPs), could be used to catalyze the reduction of nitroarenes at room temperature. Only two weight percent of our designer surfactant TPGS-750-M in water was needed to generate nanomicelles that serve as the reaction medium, with NaBH₄ as the stoichiometric source of hydride. Due to the extremely low palladium loading, we endeavoured to further enhance the activity of this catalyst (Fe/ppm Pd NPs), especially with highly functionalized substrates. Therefore, a far more reactive and functional group tolerant catalyst was sought that would minimize reaction times, of particular interest to reactions run at scale.

Results and discussion

Our initial study began with replacement of the Pd present in the NPs with varying amounts of Ni salts, with best results

^aDepartment of Chemistry and Biochemistry, University of California, Santa Barbara, California 93106, USA. E-mail: lipshutz@chem.ucsb.edu

^bNovartis Pharma AG, Basel, Switzerland

^cChemical Sciences and Engineering Division, Argonne National Laboratory, Lemont, IL 60439, USA

†Electronic supplementary information (ESI) available. See DOI: 10.1039/c7gc02991h

obtained using $\text{Ni}(\text{NO}_3)_2 \cdot 6\text{H}_2\text{O}$ (Fig. 1). Reagent optimization studies revealed a dependence on two key variables in addition to the nickel(II) source: (1) the equivalents of MeMgCl used to form the NPs, and (2) the amount of NaBH_4 used for catalyst activation (see the ESI, Tables S1 to S5†). Using 4-chloronitrobenzene as a model substrate, reaction with Fe/ppm Ni NPs was surprisingly slower (12 h) than the corresponding reaction using Fe/ppm Pd NPs (2 h; Table 1). Remarkably, preparing the same NPs containing both 80 ppm Pd, 1600 ppm Ni and 2 mol% Fe led to complete conversion in 15 minutes. Additional examples, as illustrated in Table 2, attest to this same trend. Fe NPs prepared from pure FeCl_3 in the absence of both Pd and Ni led to a very slow reaction (19% product after 14 h).

Following reduction with MeMgCl , the mixture was quenched with pentanes containing traces of water, and then triturated by additional pentanes to afford khaki-colored Fe/ppm Pd + Ni NPs (Fig. 1). The nanoparticles could be used directly upon activation with NaBH_4 (Fig. 2), or isolated and stored in solid form, without loss of activity, for several months at room temperature and without protection from air. Should these NPs turn from yellow-brown to orange upon exposure to air over time, there is no loss in activity since the NaBH_4 in the pot quickly converts them back to their active form. This process could be further streamlined by taking advantage of the recently disclosed co-solvent effect,²⁰ in these cases using 10% THF. As revealed by each of the five additional

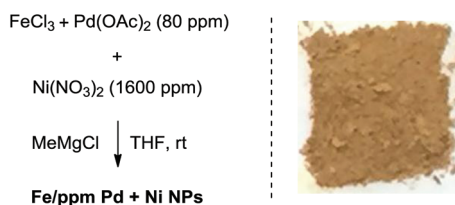


Fig. 1 Generation and appearance of iron nanoparticles containing ppm levels of Pd and Ni.

Table 1 Comparison of rates of reduction by NPs in water

Nanoparticles (NPs)	Yield (%)	Time
Fe/ppm Pd NPs	90	2 h
Fe/ppm Ni NPs ^a	79	12 h
Fe/ppm Pd + Ni NPs^b	96	15 min

^a $\text{Ni}(\text{NO}_3)_2 \cdot 6\text{H}_2\text{O}$ as Ni source, 1600 ppm Ni. ^b $\text{Ni}(\text{NO}_3)_2 \cdot 6\text{H}_2\text{O}$ as Ni source; 1600 ppm Ni, 80 ppm Pd.

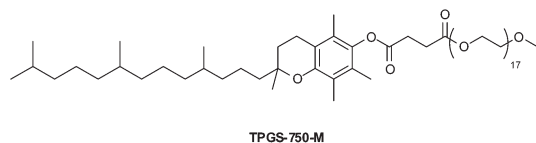
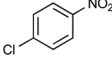
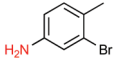
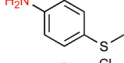
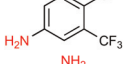
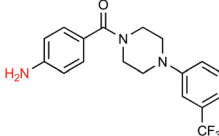


Table 2 Comparison between Fe/ppm Pd + Ni NPs and NPs of Fe/ppm Pd (without Ni)

Substrate	Fe/ppm Pd + Ni ^a		Fe/ppm Pd	
	Time	Yield ^b	Time	Yield ^b
				
	30 min	98%	90 min	96%
	2 h	88%	12 h	72%
	30 min	98%	2 h	94%
	30 min	99%	2 h	98%
	2 h	88%	8 h	90%

^a Ni source: $\text{Ni}(\text{NO}_3)_2 \cdot 6\text{H}_2\text{O}$, MeMgCl : 1.27 equiv. ^b Isolated yield.



Fig. 2 Generation (A) and appearance, after exposure to NaBH_4 ; (B) of iron nanoparticles containing ppm levels of Pd and Ni.

examples illustrated in Table 2, the rates of reduction could be increased significantly.

Analyses of the active NPs by transmission electron microscopy (TEM), using a copper grid, in 2 wt% TPGS-750-M aqueous solutions show spherical particles (Fig. 3). As seen previously,²¹ these metal NPs are associated with existing nanomicelles in aqueous solution due to the presence of (M) PEG within the surfactant. Energy Dispersive X-Ray (EDX) data (Fig. 4) for the same nanoparticles indicate that the ratio of Fe/Ni is 12.3, which is close to the theoretical ratio of 11.9 (see the detailed calculation in ESI 5b†). The presence of palladium at these low levels, as expected,¹⁹ was not observed.

To assess the scope of this technology, an expansive study was undertaken examining several types of nitroarenes and -heteroarenes. Under standard conditions (*i.e.*, 2 wt%

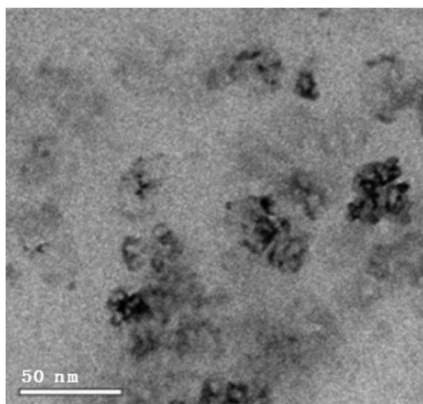


Fig. 3 Catalyst characterization by cryo-TEM of Fe/ppm Pd + Ni NPs in aqueous TPGS-750-M after adding NaBH₄.

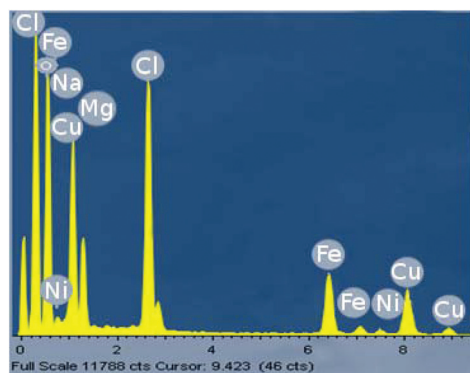


Fig. 4 EDX for Fe/ppm Pd + Ni NPs in the presence of NaBH₄.

TPGS-750-M/H₂O, NaBH₄ (3 equiv.), 10% THF co-solvent at room temperature), most reactions took place quite smoothly and in excellent yields (Table 3). Products containing substituents on the aromatic/heteroaromatic ring, including fluoro-(10), chloro-(1, 4), bromo-(2, 7, 10, 14), trifluoromethyl-(12, 17, 18), chlorodifluoromethoxy-(23), were formed without incident. Reduction in the presence of other functionality, such as ester, amide, sulfonyl-, thio-, hydrazinyl-, as well as C–C double bonds, likewise, occurred smoothly. Heterocycles including pyridine, isoxazole, quinoline, piperazine, piperidine, morpholine were all tolerated, strongly suggesting potential applications to targets in the pharmaceutical and agrochemical arenas. By contrast, reactions run under identical conditions but in pure THF were extremely slow, with 4-chloronitrobenzene affording the targeted product to the extent of only 27% after 16 hours.

Several of the examples studied (Table 3) presented special challenges due to the nature of nitro compounds that can be highly crystalline, and/or flocculent solids and therefore, slow to gain entry to the inner micellar cores. Practical issues, such as an adherence to the stir bar, or formation of insoluble gums, were readily solved by the presence of varying amounts of a co-solvent. While THF was the first co-solvent to be chosen (see products 14, 18, 20, 25, 27), varying percentage of other water-miscible co-solvents such as MeOH (see 16) and DMSO (see

13, 19, 22, 24) were found to also lead to clean overall primary amine formation. Lowering the global concentration from 0.5 to 0.25, or even 0.10 M also occasionally was beneficial (see 11, 14, 15, 16, 22, 24, 25, 26, 27, 28). Typically, NaBH₄ was used to generate the Pd–H species, although on occasion, KBH₄ led to a more effective reduction, as noted previously by Gallou and co-workers.²²

Given the increasing number of key synthetic transformations that can now be run under mild conditions in aqueous media using micellar technology,²³ sequences can be planned that take advantage of the commonality of this reaction medium. As examples that include nitro group reductions, product 27 could be formed *via* this NP-mediated reduction, after which it is then converted to its Cbz derivative 28. Final cyclization *via* a Fischer indole synthesis to 29 proceeded in good overall yield (Scheme 1).

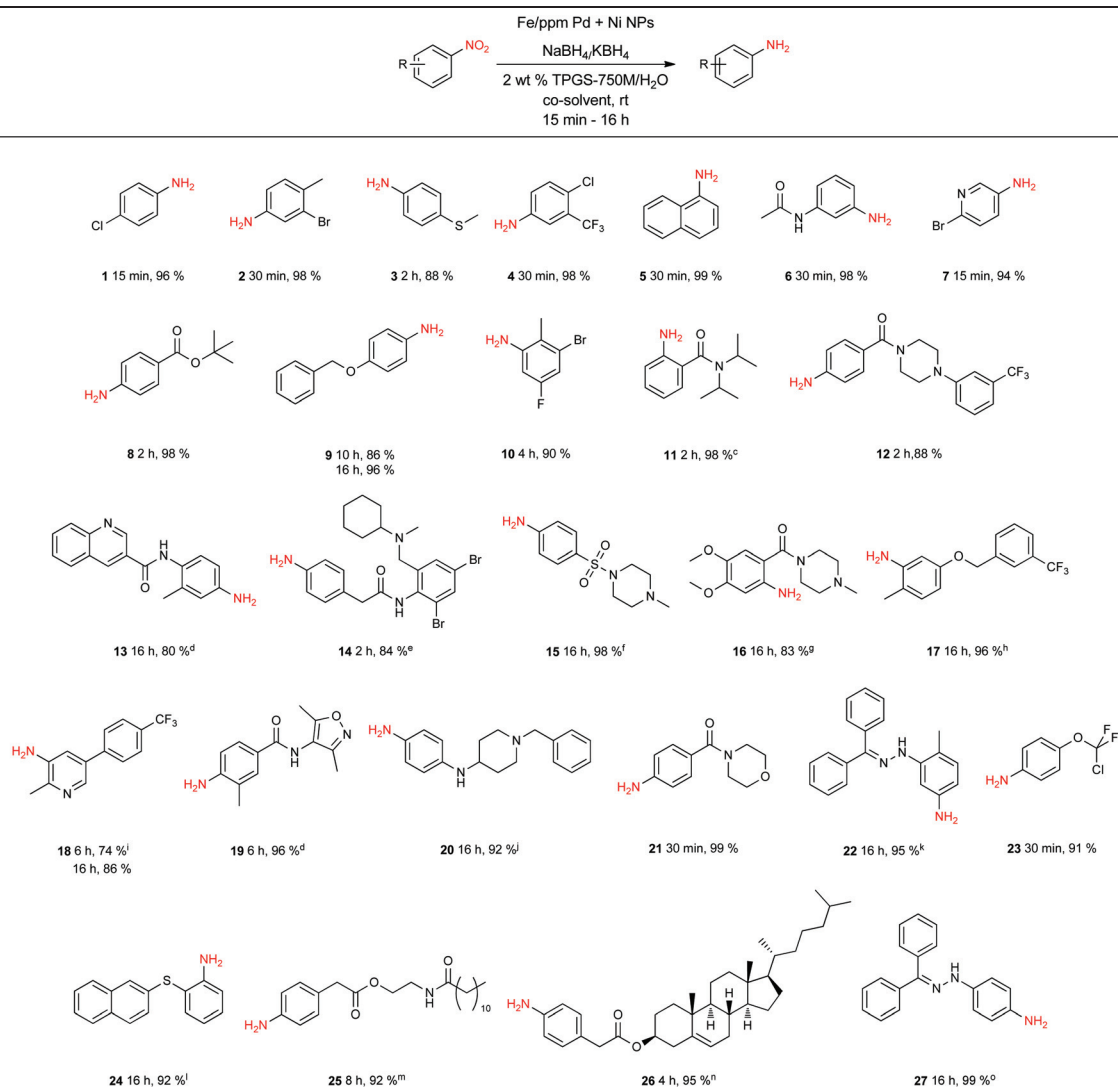
An alternative, representative 1-pot sequence, illustrated Scheme 2, converts 4-chloronitrobenzene initially to its aniline derivative. Subsequent S_NAr addition leads to adduct 30, and then a Suzuki–Miyaura coupling affords biaryl 31, all done in water between rt and 45 °C in high overall yield.

As is characteristic of designer surfactant technology in water, “in flask” recycling of an aqueous reaction mixture is straight forward.¹⁸ Thus, following reduction of a nitroaromatic (Scheme 3), extraction of the resulting substituted aniline upon addition of minimal amounts of a single organic solvent (*e.g.*, MTBE) afforded the desired product, subject to purification. The E Factor²⁴ associated with this process based on solvent usage as a measure of “greenness” is <4, which is quite low and reflects the limited solvent needed to remove the product from the reaction mixture. As THF remains partly in the aqueous phase, no additional co-solvent is needed with each recycle. Addition of fresh NPs, however, was required to ensure full conversion after an extractive workup. Yields for each of the four recycles studied remained high.

Another important aspect of this protocol concerns the amounts of residual metal to be expected in the product from reductions of nitroarenes. Established guidelines for allowable levels of transition metal impurities vary as a function of levels of toxicity.²⁵ Residual Fe is considered relatively innocuous (limit: 1300 ppm), while limits for both Ni (25 ppm) and especially Pd (10 ppm) are far more rigorous.¹⁹ Metal impurities that exceed these levels require additional time, effort, and cost to have them removed or at least, reduced to allowable levels.

Analyses were conducted on several products resulting from Fe/ppm Pd + Ni NP-catalyzed nitro group reductions by inductively coupled plasma mass spectrometry (ICP-MS). Results (see ESI†) showed residual palladium to be below 10 ppm, while residual nickel was below 1 ppm. Residual iron was also measured and found to be below 5 ppm, implying in the composite that release of any metal from these NPs is minimal.

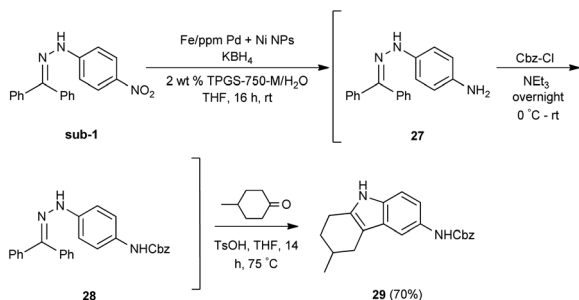
The role played by the added Ni in enhancing reactivity of the *in situ*-formed palladium hydride can be initially ascertained *via* XAS experiments on the activated catalysts, Fe/ppm

Table 3 Representative reductions of nitroarenes^{a,b}

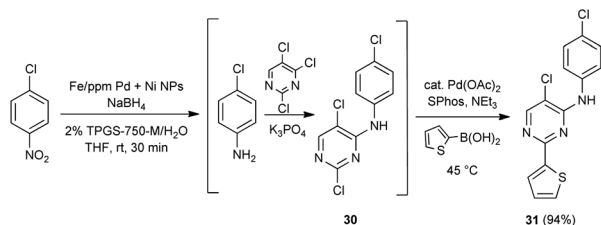
^a Reaction conditions: Nitro compound (0.5 mmol), Fe nanoparticles (6 mg, 2% Fe, 80 ppm Pd, 1600 ppm Ni), NaBH₄ (1.5 mmol), 2 wt% TPGS-750-M/H₂O (1 mL), THF (0.1 mL). ^b Isolated yield. ^c Nitro compound (0.125 mmol), Fe nanoparticles (3 mg), NaBH₄ (0.375 mmol), 2 wt% TPGS-750-M/H₂O (1 mL), THF (0.1 mL). ^d DMSO (0.25 mL). ^e Nitro compound (0.125 mmol), Fe nanoparticles (3 mg), NaBH₄ (0.375 mmol), 2 wt% TPGS-750-M/H₂O (1 mL), THF (0.3 mL). ^f Nitro compound (0.25 mmol), Fe nanoparticles (3 mg), NaBH₄ (0.75 mmol), TPGS-750-M/H₂O (1 mL), THF (0.1 mL). ^g Nitro compound (0.25 mmol), Fe nanoparticles (3 mg), NaBH₄ (0.75 mmol), TPGS-750-M/H₂O (1 mL), CH₃OH (0.25 mL). ^h Nitro compound (0.5 mmol), Fe nanoparticles (12 mg), NaBH₄ (3 mmol), 2 wt% TPGS-750-M/H₂O (1 mL), DCM (0.1 mL). ⁱ THF (0.25 mL). ^j Nitro compound (0.125 mmol), Fe nanoparticles (1.5 mg), KBH₄ (0.375 mmol), 2 wt% TPGS-750-M/H₂O (1 mL), THF (0.25 mL). ^k Nitro compound (0.125 mmol), Fe nanoparticles (2.5 mg), KBH₄ (0.75 mmol), 2 wt% TPGS-750-M/H₂O (1 mL), DMSO (0.25 mL). ^l Nitro compound (0.125 mmol), Fe nanoparticles (2.5 mg), KBH₄ (0.75 mmol), 2 wt% TPGS-750-M/H₂O (1 mL), DMSO (0.25 mL). ^m Nitro compound (0.25 mmol), Fe nanoparticles (2.5 mg), KBH₄ (0.75 mmol), 2 wt% TPGS-750-M/H₂O (1 mL), THF (0.25 mL). ⁿ Nitro compound (0.25 mmol), Fe nanoparticles (3 mg), NaBH₄ (0.75 mmol), 2 wt% TPGS-750-M/H₂O (1 mL), DCM (0.3 mL). ^o Nitro compound (0.125 mmol), Fe nanoparticles (1.5 mg), KBH₄ (0.75 mmol), 2 wt% TPGS-750-M/H₂O (1 mL), THF (0.25 mL).

Pd and Fe/ppm Pd + Ni. On the basis of EXAFS data, a higher shell scattering feature attributed to Pd–Pd interactions and the presence of Pd oligomers was observed for the Fe/ppm Pd system. Such a feature was not observed in the presence of Ni (see ESI†), indicating that Ni dilutes the palladium content on the surface of these NPs, leading to increased Pd dispersity and thereby, increasing the reactivity of the isolated palladium atoms.²⁶ More definitive imaging techniques such as aberration-

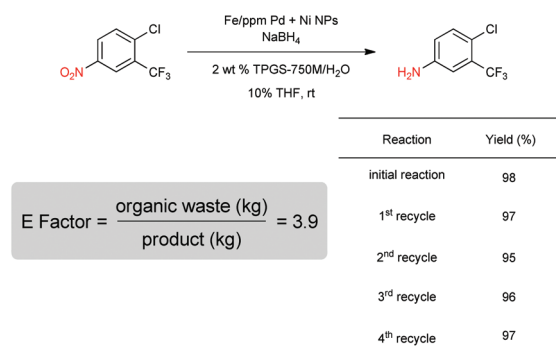
corrected HAADF STEM would be needed to establish Pd site isolation in the presence of Ni, and these experiments are presently under consideration. That a base metal such as nickel can be used to enhance the reactivity of a precious metal within a nanoparticle catalyst, leading to greater activity notwithstanding the ppm levels involved, is an exciting discovery that may have a considerable number of applications to other types of precious metal catalysis.



Scheme 1 1-Pot nitro group reduction followed by amine protection and Fischer indole synthesis.



Scheme 2 1-Pot, 3-step sequence involving NO_2 group reduction / $\text{S}_{\text{N}}\text{Ar}$ /Suzuki–Miyaura coupling, in water.



Scheme 3 Studies on recycling and determination of E factor.

Conclusion

In summary, a new catalyst useful for nitro group reductions in water has been uncovered that contains ppm levels of both Pd and Ni that work in harmony to afford greater reactivity than that observed using related catalysts based on either individual metal. The process is safe, takes place in water under mild conditions, and allows for facile in-flask product isolation as well as recycling of the entire aqueous reaction mixture. Very low levels of residual metals are found in the isolated products, further enhancing the attractiveness of this environmentally responsible technology.

Conflicts of interest

The authors declare no conflicts of interest.

Acknowledgements

Financial support provided by Novartis and the NSF (SusChEM 1566212) is warmly acknowledged with thanks. Work at Argonne National Laboratory is supported by the U.S. Department of Energy (DOE), Office of Basic Energy Sciences, Division of Chemical Sciences, Biosciences and Geosciences under Contract DE-AC02-06CH11357. Use of the Advanced Photon Source at Argonne National Laboratory is supported by the U.S. Department of Energy, Office of Science, and Office of Basic Energy Sciences, under Contract DE-AC02-06CH11357. MRCAT operations are supported by the Department of Energy and the MRCAT member institutions.

Notes and references

- (a) S. De, J. Zhang, R. Luque and N. Yan, *Energy Environ. Sci.*, 2016, **9**, 3314–3347; (b) M. Delferro and T. J. Marks, *Chem. Rev.*, 2011, **111**, 2450–2485.
- D. R. Pye and N. P. Mankad, *Chem. Sci.*, 2017, **8**, 1705–1718.
- C. Parmeggiani, C. Matassini and F. Cardona, *Green Chem.*, 2017, **19**, 2030.
- (a) P. T. Anastas and J. C. Warner, *Green Chemistry: Theory and Practice*, Oxford University Press, 1998; (b) P. Anastas and N. Eghbali, *Chem. Soc. Rev.*, 2010, **39**, 301.
- (a) A. M. Birch, S. Groombridge, R. Law, A. G. Leach, C. D. Mee and C. Schramm, *J. Med. Chem.*, 2012, **55**, 3923; (b) R. S. Downing, P. J. Kunkeler and H. van Bekkum, *Catal. Today*, 1997, **37**, 121–136; (c) H.-U. Blaser, H. Steiner and M. Studer, *ChemCatChem*, 2009, **1**, 210.
- M. Orlandi, D. Brenna, R. Harms, S. Jost and M. Benaglia, *Org. Process Res. Dev.*, 2016, DOI: 10.1021/acs.oprd.6b00205.
- (a) M. M. Dell'Anna, S. Intini, G. Romanazzi, A. Rizzuti, C. Leonelli, F. Piccinni and P. Mastroianni, *J. Mol. Catal. A: Chem.*, 2014, **395**, 307; (b) A. Chinnappan and H. Kim, *RSC Adv.*, 2013, **3**, 3399; (c) O. Verho, K. P. J. Gustafson, A. Nagendiran, C.-W. Tai and J.-E. Bäckvall, *ChemCatChem*, 2014, **6**, 3153.
- L. He, L.-C. Wang, H. Sun, J. Ni, Y. Cao, H.-Y. He and K.-N. Fan, *Angew. Chem., Int. Ed.*, 2009, **48**, 9538.
- S. G. Oh, V. Mishra, J. K. Cho, B.-J. Kim, H. S. Kim, Y.-W. Suh, H. Lee, H. S. Park and Y. J. Kim, *Catal. Commun.*, 2014, **43**, 79.
- (a) E. H. Boymans, P. T. Witte and D. Vogt, *Catal. Sci. Technol.*, 2015, **5**, 176; (b) H. Wei, X. Liu, A. Wang, L. Zhang, B. Qiao, X. Yang, Y. Huang, S. Miao, J. Liu and T. Zhang, *Nat. Commun.*, 2014, **5**, 5634; (c) B. Zhang, H. Asakura, J. Zhang, J. Zhang, S. De and N. Yan, *Angew. Chem., Int. Ed.*, 2016, **55**, 8319–8323.
- N. Sakai, S. Asama, T. Konakahara and Y. Ogiwara, *Synthesis*, 2015, **47**, 3179.
- (a) F. A. Westerhaus, R. V. Jagadeesh, G. Wienhöfer, M.-M. Pohl, J. Radnik, A.-E. Surkus, J. Rabeah, K. Junge,

- H. Junge, M. Nielsen, A. Brückner and M. Beller, *Nat. Chem.*, 2013, **5**, 537; (b) R. K. Rai, A. Mahata, S. Mukhopadhyay, S. Gupta, P.-Z. Li, K. T. Nguyen, Y. Zhao, B. Pathak and S. K. Singh, *Inorg. Chem.*, 2014, **53**, 2904; (c) R. V. Jagadeesh, D. Banerjee, P. B. Arockiam, H. Junge, K. Junge, M.-M. Pohl, J. Radnik, A. Bruckner and M. Beller, *Green Chem.*, 2015, **17**, 898.
- 13 (a) R. J. Kalbasi, A. A. Nourbakhsh and F. Babaknezhad, *Catal. Commun.*, 2011, **12**, 955; (b) O. Mazaheri and R. J. Kalbasi, *RSC Adv.*, 2015, **5**, 34398; (c) A. Chinnappan and H. Kim, *RSC Adv.*, 2013, **3**, 3399.
- 14 E. Pedrajas, I. Sorribes, A. L. Gushchin, Y. A. Laricheva, K. Junge, M. Beller and R. Llusar, *ChemCatChem*, 2017, **9**, 1128.
- 15 S. M. Kelly and B. H. Lipshutz, *Org. Lett.*, 2014, **16**, 98.
- 16 M. L. Di Gioia, A. Leggio, I. F. Guarino, V. Leotta, E. Romio and A. Liguori, *Tetrahedron Lett.*, 2015, **56**, 5341.
- 17 (a) A. J. MacNair, M.-M. Tran, J. E. Nelson, G. U. Sloan, A. Ironmonger and S. P. Thomas, *Org. Biomol. Chem.*, 2014, **12**, 5082; (b) R. V. Jagadeesh, G. Wienhofer, F. A. Westerhaus, A.-E. Surkus, M.-M. Pohl, H. Junge, K. Junge and M. Beller, *Chem. Commun.*, 2011, **47**, 10972; (c) K. Junge, B. Wendt, N. Shaikh and M. Beller, *Chem. Commun.*, 2010, **46**, 1769.
- 18 B. H. Lipshutz, N. A. Isley, J. C. Fennewald and E. D. Slack, *Angew. Chem., Int. Ed.*, 2013, **52**, 10911.
- 19 J. Feng, S. Handa, F. Gallou and B. H. Lipshutz, *Angew. Chem., Int. Ed.*, 2016, **55**, 8979.
- 20 C. M. Gabriel, N. R. Lee, F. Bigorne, P. Klumphu, M. Parmentier, F. Gallou and B. H. Lipshutz, *Org. Lett.*, 2017, **19**, 194.
- 21 E. D. Slack, C. M. Gabriel and B. H. Lipshutz, *Angew. Chem., Int. Ed.*, 2014, **53**, 14051.
- 22 (a) C. M. Gabriel, M. Parmentier, C. Riegert, M. Lanz, S. Handa, B. H. Lipshutz and F. Gallou, *Org. Process Res. Dev.*, 2017, **21**, 247; (b) See also M. Orlandi, D. Brenna, R. Harms, S. Jost and M. Benaglia, *Org. Process Res. Dev.*, 2016, DOI: 10.1021/acs.oprd.6b00205.
- 23 (a) B. H. Lipshutz and S. Ghorai, *Green Chem.*, 2014, **16**, 3660–3679; (b) B. H. Lipshutz, *Johnson Matthey Technol. Rev.*, 2017, **61**, 196.
- 24 (a) R. A. Sheldon, I. W. C. E. Arends and U. Hanefeld, *Green Chemistry and Catalysis*, Wiley-VCH, Weinheim, 2007, pp. 1–47; (b) R. A. Sheldon, *Green Chem.*, 2007, **9**, 1273.
- 25 Committee For Medicinal Products For Human Use (CHMP), *Guideline On The Specification Limits For Residues Of Metal Catalysts Or Metal Reagents*, European Medicines Agency, London, 2008.
- 26 (a) J. Qu, X. Zhou, F. Xu, X.-Q. Gong and S. C. E. Tsang, *J. Phys. Chem. C*, 2014, **118**, 24452; (b) G. Liu, L. Zeng, Z.-J. Zhao, H. Tian, T. Wu and J. Gong, *ACS Catal.*, 2016, **6**, 2158; (c) L. Shi, G.-M. Deng, W.-C. Li, S. Miao, Q.-N. Wang, W.-P. Zhang and A.-H. Lu, *Angew. Chem., Int. Ed.*, 2015, **54**, 13994; (d) B. Qiao, A. Wang, X. Yang, L. F. Allard, Z. Jiang, Y. Cui, J. Liu, J. Li and T. Zhang, *Nat. Chem.*, 2011, **3**, 634.